Science Advances
AAAS

Supplementary Materials for

Generalizable and replicable brain-based predictions of cognitive functioning across common psychiatric illness

Sidhant Chopra *et al.*

Corresponding author: Sidhant Chopra, sidhantchopra4@gmail.com

Sci. Adv. **10**, eadn1862 (2024)
DOI: 10.1126/sciadv.adn1862

This PDF file includes:

Supplementary Table 1 – Sample demographics

	HCP-EP (n=145)	**TCP** (n=101)	**CNP** (n=224)
Age *(mean,sd)*	*23.41(3.86)*	*32.21(12.54)*	*32.59(9.21)*
Sex *(f, %)*	*57, 38%*	*50, 57%*	*95, 42%*
Head motion *(mm, sd)*	*.06(.04)*	*.09(.05)*	*.08(.03)*
Diagnosis			
*SZ**	*62*	*4*	*37*
SZAD	*8*	*3*	*0*
MDD	*5*	*22*	*0*
BD	*20*	*9*	*40*
*ANX**	*0*	*5*	*0*
ADHD	*0*	*0*	*37*
OCD	*0*	*0*	*0*
PTSD	*0*	*7*	*0*
SUD	*1*	*1*	*0*
ED	*0*	*2*	*0*
None (HC)	*52*	*48*	*110*

Acronyms: HCP-EP = Human Connectome Project – Early Psychosis, TCP = Transdiagnostic Connectomes Project, CNP = UCLA Consortium for Neuropsychiatric Phenomics, SZ = Schizophrenia, SZAD = Schizoaffective Disorder, MDD = Major Depressive Disorder, BD = Bipolar Disorder, ANX=Anxiety Disorder, ADHD = Attention Deficit Hyperactivity Disorder, OCD = obsessive Compulsive Disorder, PTSD = Post-Traumatic Stress Disorder, SUD = Substance Use Disorder, HC = Healthy Control.

***Includes all Schizophrenia Spectrum Diagnosis, except Schizoaffective Disorder*

**Includes Generalized Anxiety Disorder and Specific Phobia*

Supplementary Table 2 - Cognitive tests for each clinical dataset and loadings on the first principal component.

HCP-EP	**loading**	**TCP**	**loading**	**CNP**
nih_picseq_unadjusted	0.230	choice_rt_score*	0.282	cvlt_sd_free_recall
nih_dccs_unadjusted	0.222	cont_concent_score*	-0.028	cvlt_sd_cued_recall
nih_flanker_unadjusted	0.235	digit_symbol_score*	0.474	cvlt_ld_free_recall
nih_tpvt_uss	0.275	fast_react_score*	0.439	cvlt_ld_cued_recall
nih_patterncomp_unadjusted	0.161	matrix_reasonscore*	0.348	cvlt_ld_recognition
nih_lswmt_uss	0.261	read_mind_score*	0.227	wms_vr_immediate_recall
nih_orrt_tbx_reading_score	0.267	recog_emo_score*	-0.011	wms_vr_delayed_recall
nih_fluidcogcomp_unadjusted	0.304	hammer_tot_meanRT^	-0.453	wms_vr_recognition
nih_crycogcomp_unadjusted	0.292	stroop_tot_meanRT^	-0.352	wms_symbol_span
nih_eccogcomp_unadjusted	0.328			wms_digit_span_fwd
nih_totalcogcomp_unadjusted	0.346			wms_digit_span_bwd
wasi_profilesubtest_verbalv	0.248			wms_digit_span_seq
wasi_profilesubtest_performancemr	0.230			wais_letter_number_sequ
wasi_iqscores_full2iq	0.289			wais_vocabulary
				wais_matrix_reasoning
				dkefs_verbal_fluency_engl
				taskswitch_interference
				taskswitch_switch_cost
				taskswitch_residual_switch
				ant_rt_conflict
				color_trail_interference
				cpt_hit_rate
				cpt_false_alarm_rate
				cpt_hits_rt

*Administered online
^Administered within MRI scanner

Supplement Table 3 – 67 Phenotypes from Biobank used to train meta-matching model

Variable	Description	Variable	Description	Variable	Description
Alcohol C3	average weekly beer plus cider intake	Trail-o C4	trail making online principal component 4	Matrix C2	matrix pattern completion principal component 2
Blood C2	blood assays principal component 2	Blood C4	blood assays principal component 4	Fluid Int.	fluid intelligence
Breath C1	spirometry principal component 1	Alcohol C2	average weekly champagne plus white wine intake	Hearing	hearing signal-to-noise-ratio (snr) of triplet (left)
Age	age	Carotid C5	carotid ultrasound principal component 5	Illness C1	non-cancer illness principal component 1
Cancer C1	cancer principal component 1	Time drive	time spent driving per day	#household	number of people in household
Carotid C1	carotid ultrasound principal component 1	Travel	frequency of travelling from home to job	Time TV	time spent watching television (tv) per day

			workplace per week		
Match-o	pairs matching online	Work	weekly length of working hour for main job	BP eye C2	blood pressure & eye measures component 2
Trail C1	trail making principal component 1	Age edu	age completed full time education	Body C3	anthropometry principal component 3
Digit-o C1	symbol digit substitution online principal component 1	Deprive C1	multiple deprivation principal component 1	ECG C6	ECG measures principal component 6
Digit C1	symbol digit substitution principal component 1	Blood C3	blood assays principal component 3	ECG C2	ECG measures principal component 2
Match	pairs matching	Alcohol C1	average monthly spirits intake	Illness C4	non-cancer illness principal component 4
ProMem C1	prospective memory principal component 1	Neuro	neuroticism score	Smoke C1	smoke principal component 1
RT C1	reaction time principal component 1	ECG C1	ECG measures principal component 1	BP eye C3	blood pressure & eye measures principal component 3
Trail-o C1	trail making online	Sex	sex	BP eye C6	blood pressure & eye

	principal component 1				measures principal component 6
Tower C1	tower rearranging principal component 1	Sex G C2	genotype sex inference principal component 2	Urine C1	urine assays principal component 1
Family C1	family history (parent's age) principal component 1	Body C2	anthropom etry principal component 2	Sex G C1	genotype sex inference principal component 1
Blood C5	blood assays principal component 5	Grip C1	hand grip strength principal component 1	Bone C1	bone-densitometry of heel principal component 1
Dur C4	process durations principal component 4	Body C1	anthropom etry principal component 1	Matrix C3	matrix pattern completion principal component 3
Dur C2	process durations principal component 2	Bone C3	bone-densitometry of heel principal component 3	Time walk	number of days walked 10+ minutes per week
Loc C1	location principal component 1	BP eye C4	blood pressure & eye measures principal component 4	BP eye C5	blood pressure & eye measures principal component 5
Dur C1	process durations principal	Matrix C1	matrix pattern completion principal	ECG C3	ecg measures principal

	component 1		component 1		component 3
Digit-o C6	symbol digit substitution online principal component 6	#Mem C1	numeric memory principal component 1	Genetic C1	genetic principal components and heterozygosity principal component 1
				Sleep	sleep duration per day

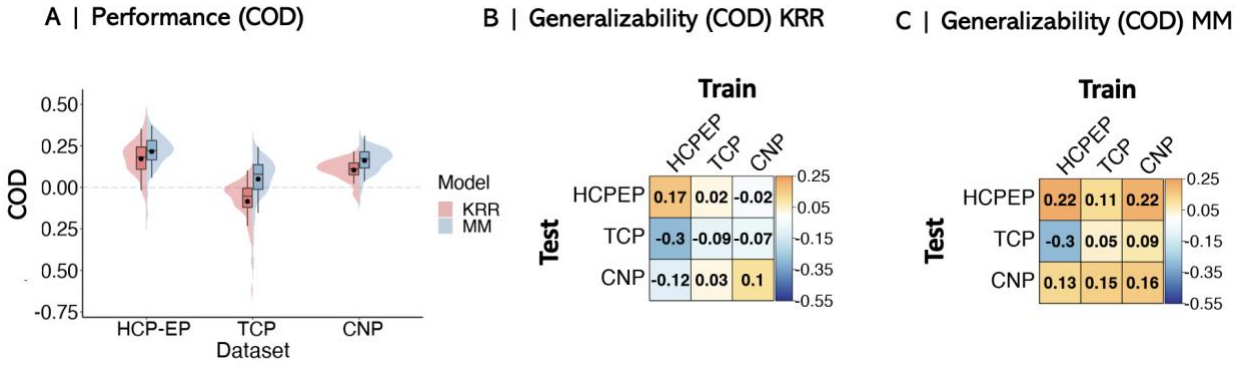

Supplementary Figure 1 – Model performance and generalizability assessed using Coefficient of Determination (COD). A) Prediction performance (COD between observed and predicted values) using kernel ridge regression (red) and meta-matching (blue) across three transdiagnostic datasets: Human Connectome Project – Early Psychosis (HCP-EP), Transdiagnostic Connectomes Project (TCP) and UCLA Consortium for Neuropsychiatric Phenomics (CNP). Generalizability matrix for the kernel ridge regression (B; KRR) and meta-matching (C; MM) models, showing the prediction performance between the independent samples, where the model is trained in one dataset and then used to make predictions in an independent dataset. The diagonal represents the mean prediction performance within each dataset, which is also represented by the black dots in panel A.

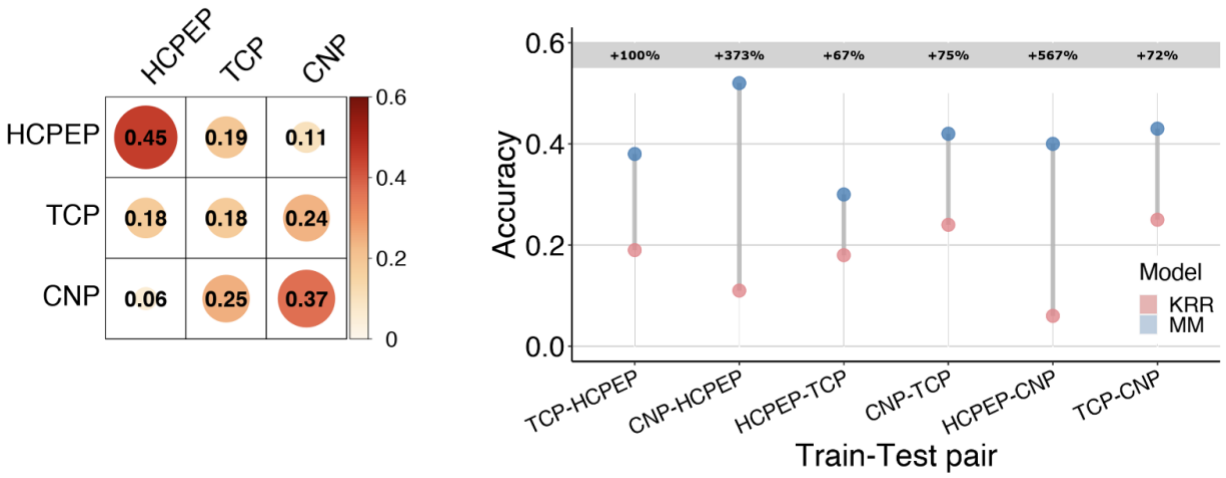

Supplementary Figure 2 – Kernel Ridge Regression (KRR) model generalizability matrix (left) and differences in generalizability between KRR and meta-matching (MM) models (right).

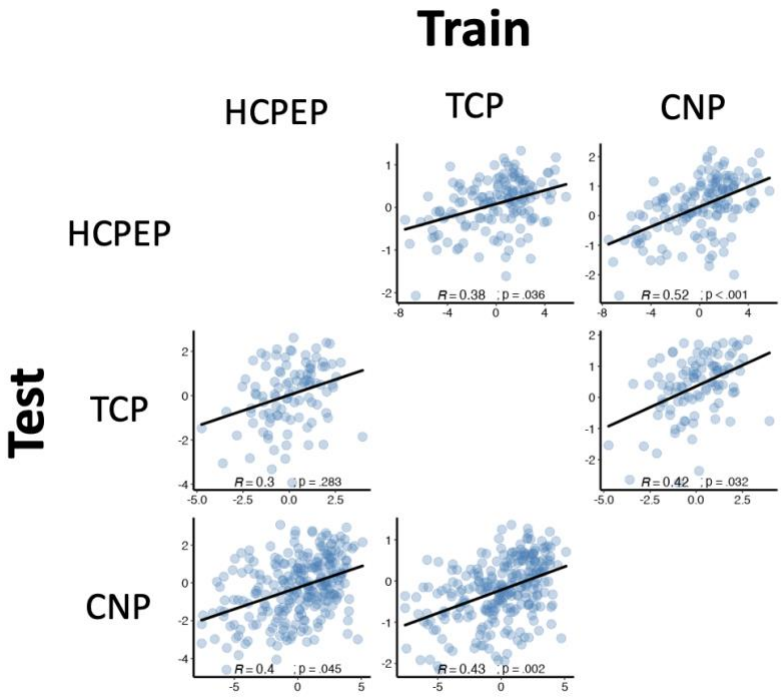

Supplementary Figure 3 – Scatterplots of observed and predicted cognition scores for generalizability of the meta-matching model.

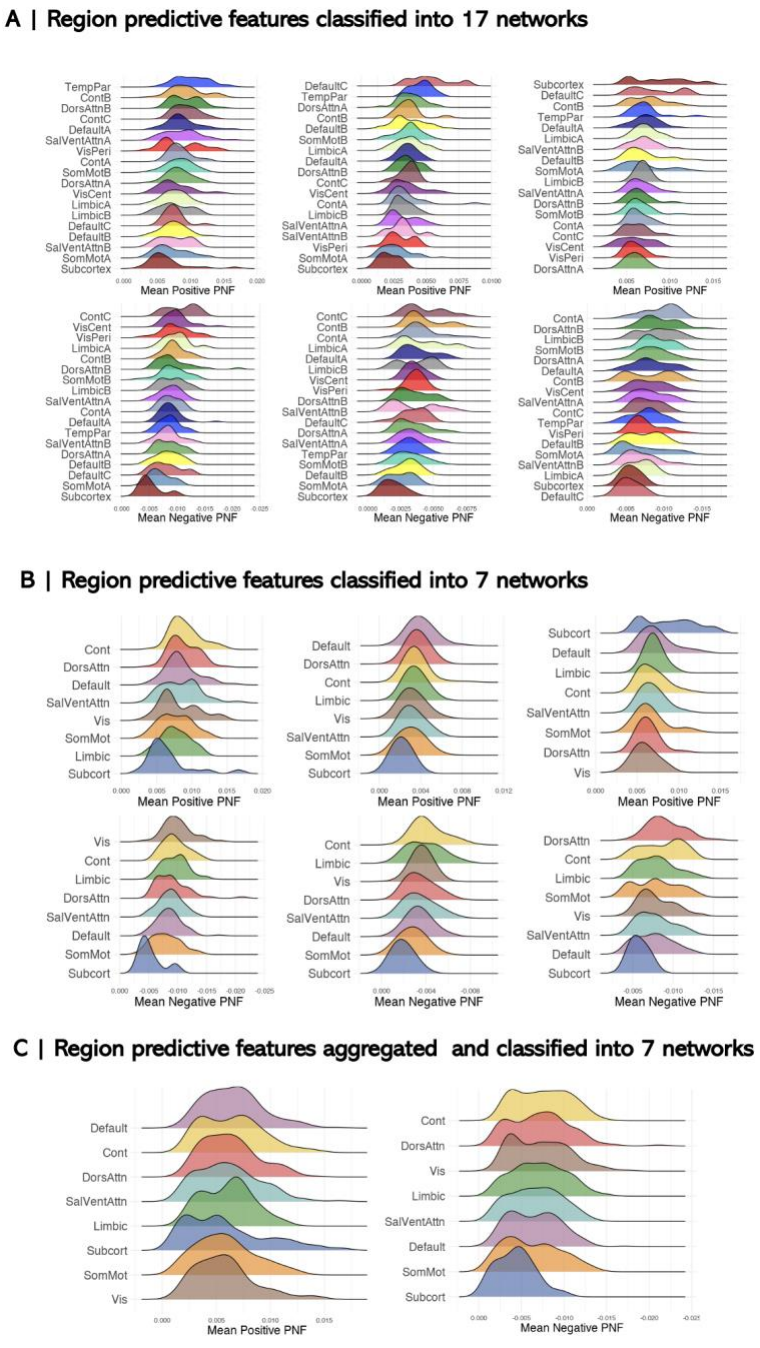

Supplementary Figure 4 – Regional predictive features classified into 17 (A) and 7 (B) network solutions, as well as aggregated across all three studies (HCP-EP, TCP, CNP) using a 7 network solution (C) and ordered by strongest to weakest mean predictive feature weight.

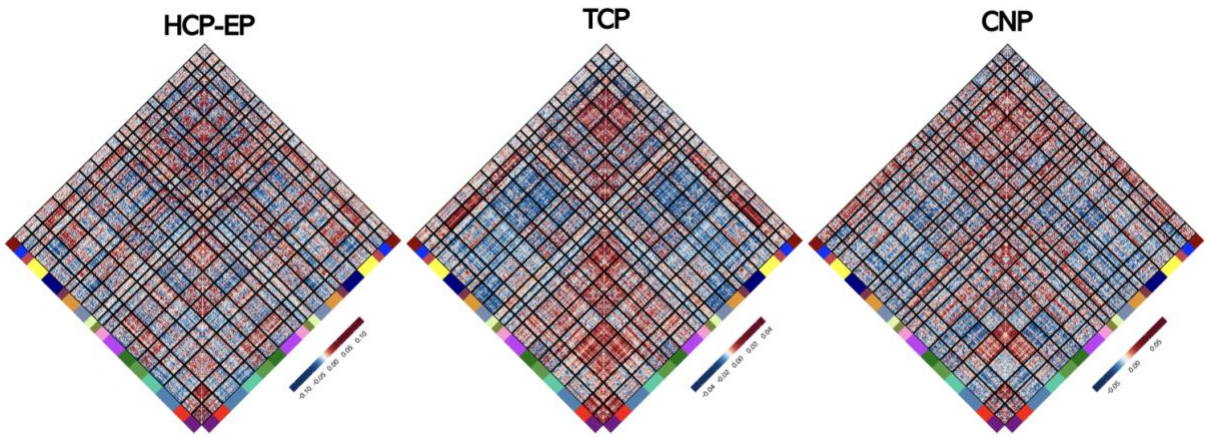

Supplementary Figure 5 – Edge-level predictive feature weights for each dataset

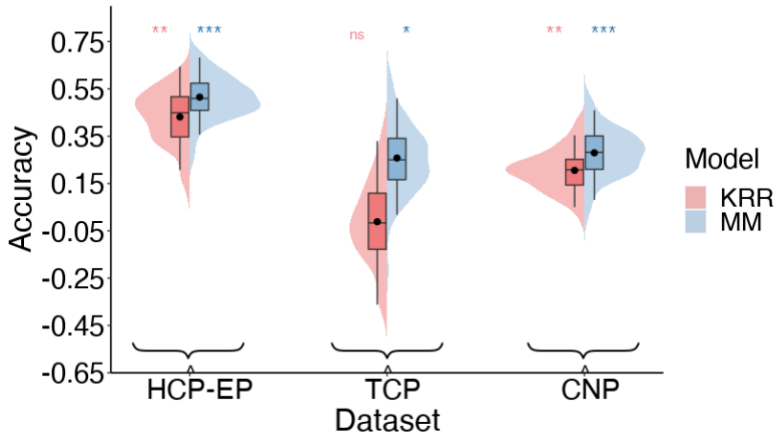

Supplementary Figure 6 - Model performance after regressing out age, sex and head motion (mean FD)

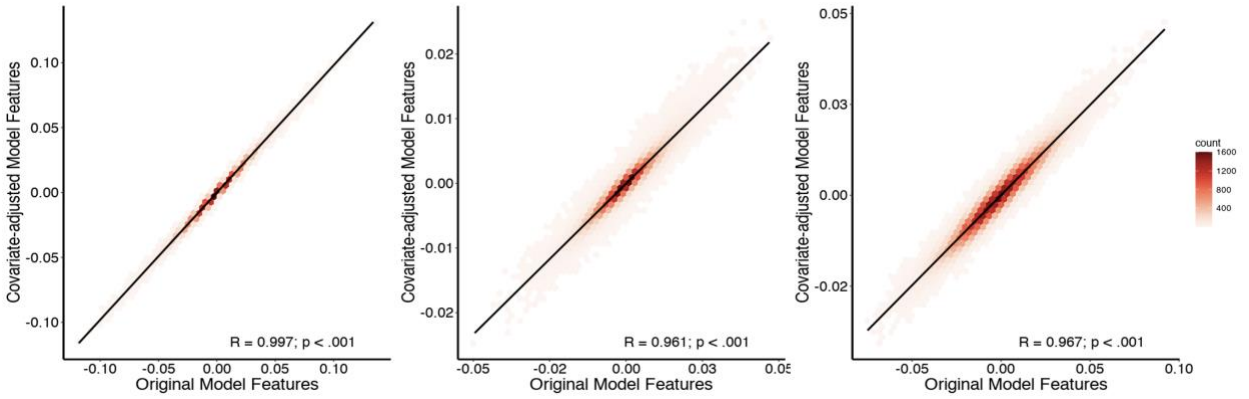

Supplementary Figure 7 - Correlation between edge-level feature weights for original and covariate adjusted meta-matching models.

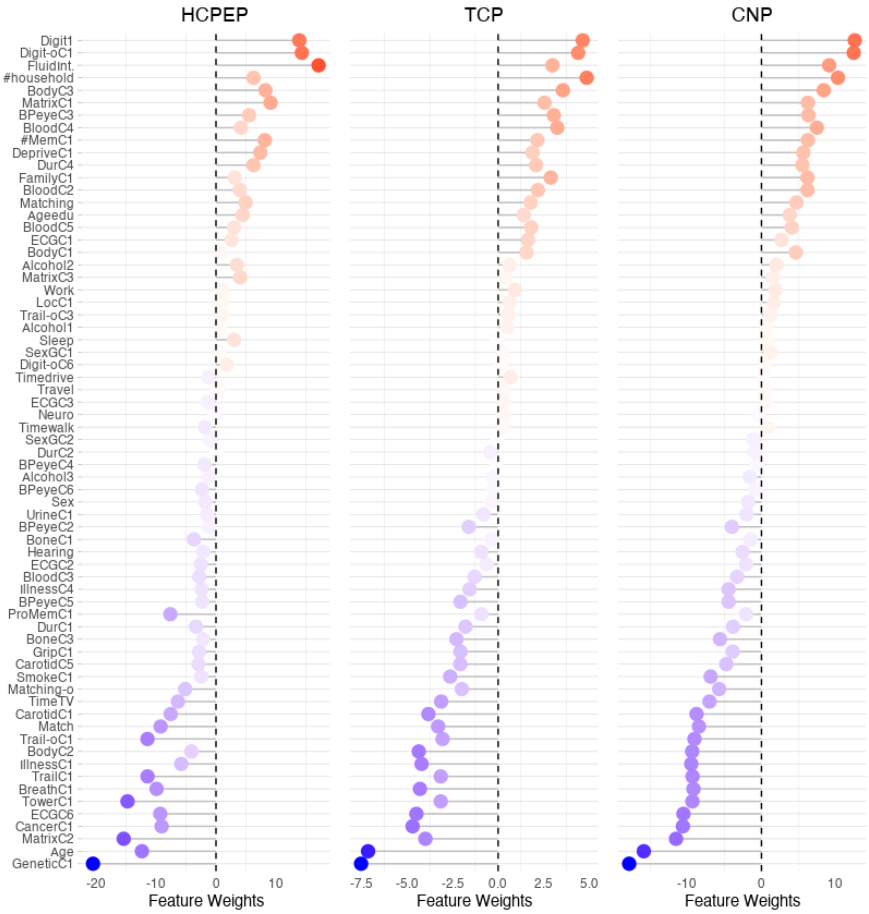

Supplementary Figure 8 –Feature weights associated with 67 health, demographic and behavioral variables using the stacking component of the meta-matching model.

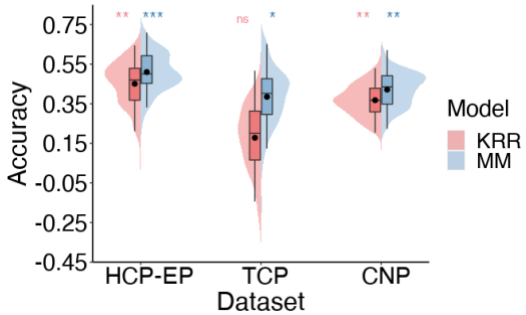

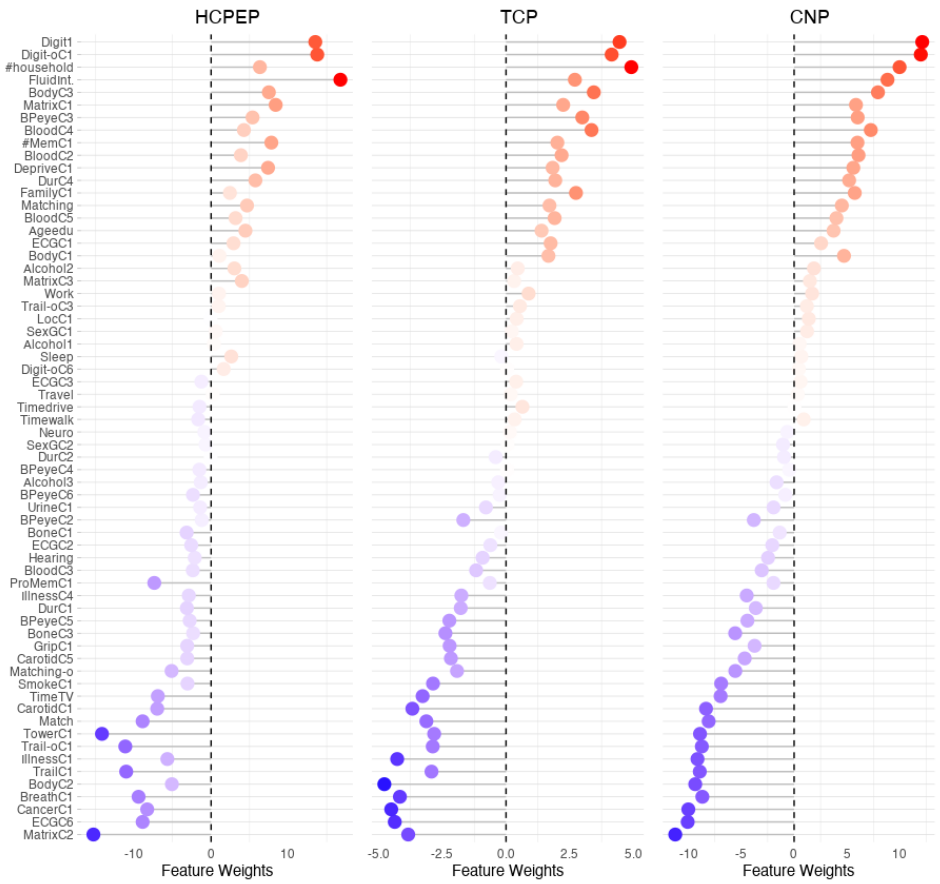

Supplementary Figure 9 – Model performance (Top) and feature weights (bottom) associated with 64 health, demographic and behavioral variables using the stacking component of the meta-matching model (after removing age, sex, and gene PC1 from the meta-matching model).

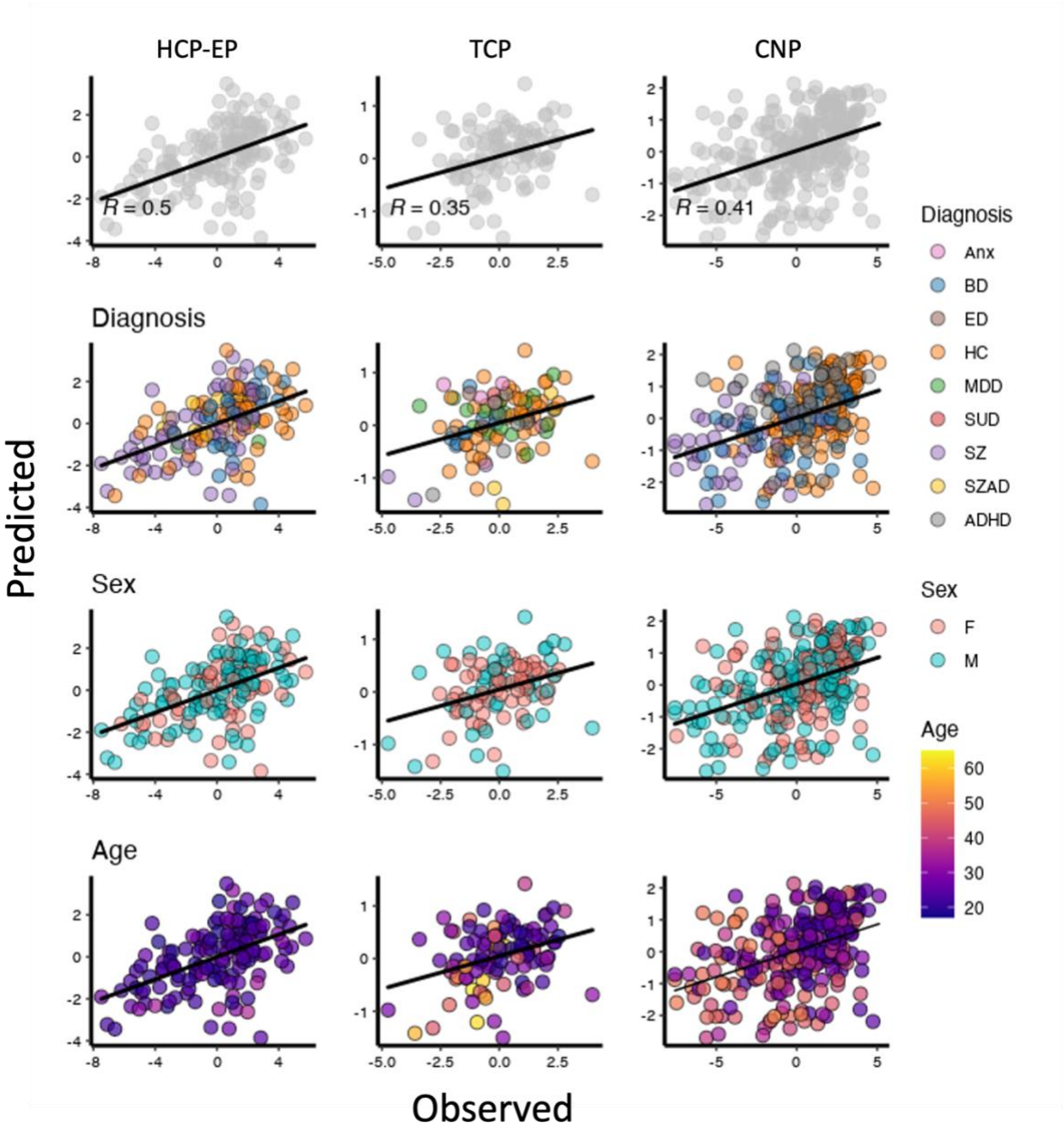

SFig10 – Leave-One Out -Cross Validation (LOO-CV) results. Points colored by diagnosis, sex, and age. F=Female; M=Male; Anx=Anxiety Disorder; BD=Bipolar Disorder; ED=Eating Disorder; HC=Healthy Control; MDD=Major Depressive Disorder; SUD=Substance Use Disorder; SZ=Schizophrenia; SZAD=Schizoaffective Disorder; ADHD=Attention Deficit Hyperactivity Disorder. See 'Control Analyses' for further details of sub-group analysis.

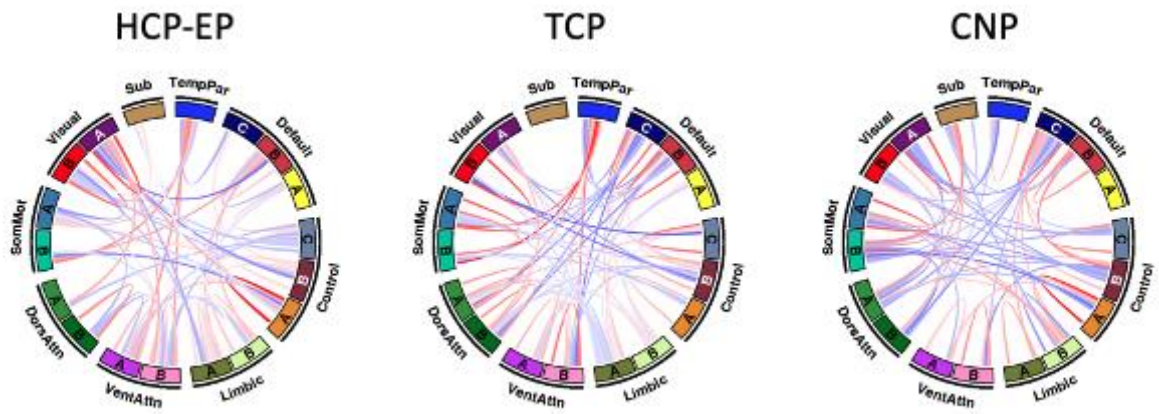

Supplementary Figure 11 – All FDR-corrected network level feature weights.

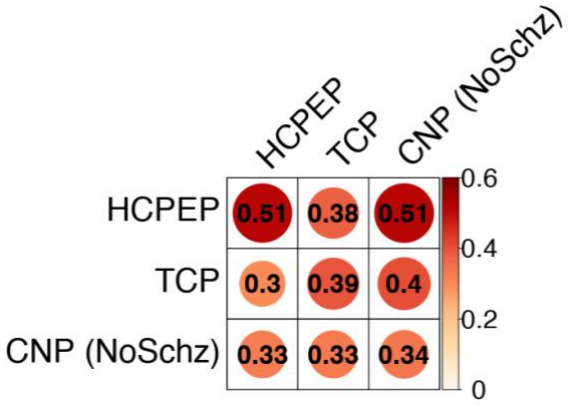

Supplementary Figure 12 – Cross-dataset generalizability after removing schizophrenia patients from CNP dataset.

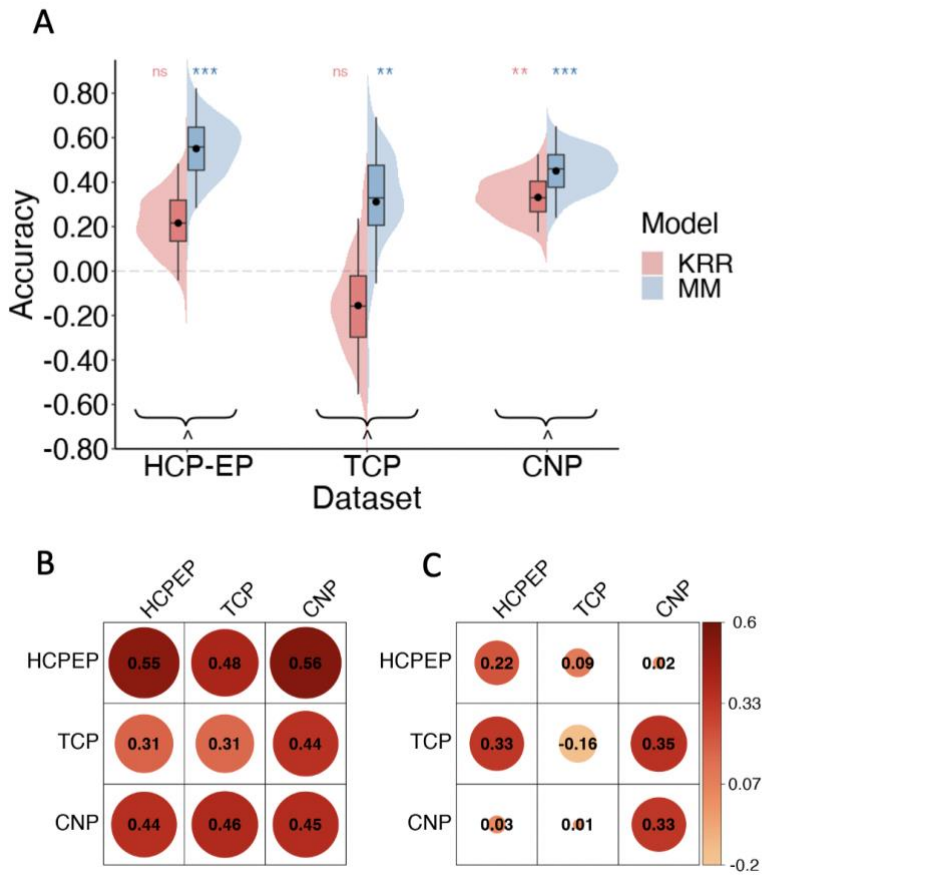

SFig 13 – A) Model performance after removing all heathy control participants from each sample. Generalizability of meta-matching (B) and KRR (C) models after removing all heathy control participants from each sample. * = p<0.05; ** = p<0.001; *** = p<0.0001; ns= p>0.05) and black ^ denotes statistically significant difference between models.

Additional Information on TCP dataset

The MRI data for the Yale University and McLean Hospital sites are collected at the FAS Brain Imaging Center and McLean Hospital Brain Imaging Center, respectively. The purpose of this study is to collect brain imaging and behavioral data from a transdiagnostic cohort of patients with common psychiatric diagnoses, as well as control participants. An open release of the TCP dataset is planned for 2024 (NDA ID: 3552). Participants are recruited from the community via flyers, online advertisements and through patient referral from clinicians. All participants complete a clinical interview and an MRI scanning session. Participants were eligible for the study if they 1) were aged between of 18-65, 2) had no MRI contraindications, 3) were not colorblind, and 4) had no neurological abnormalities. All participants underwent Structured Clinical Interview for DSM-5 to determine psychiatric diagnosis. As a result, recruitment included both healthy individuals and individuals with a diverse set of clinical presentations, including affective and psychotic psychopathology.

Additional Information on MRI processing and denoising

For the UK Biobank, we used the processed volumetric rs-fMRI data from the first imaging visit(*1*). Each fMRI dataset was spatially normalised to MNI152 2-mm template space and FMRIB's ICA-based X-noiseifier ((FSL-FIX; *2*)) was trained on holdout set of participants and applied to the remaining participants to denoise the data. The mean global signal was extracted using a whole-brain mask and was regressed out of each dataset. A detailed outline of the processing, denoising and quality control of these data has been previously reported (*1*).

For the CNP data set, *fmriprep* v1.1.1(*3*) was used. During this standardised and automated pipeline, each T1-weighted (T1w) volume was corrected for intensity non-uniformity using N4BiasFieldCorrection(*4*) and skull-stripped using antsBrainExtraction.sh. Brain surfaces were reconstructed using recon-all from FreeSurfer v6. Spatial normalization to the MNI152 Nonlinear Asymmetrical template version 2009c was performed through nonlinear registration with ANTs(*5*), using brain-extracted versions of both T1w volume and template. Brain-tissue segmentation of tissue classes was performed on the brain-extracted T1w using FSL FAST(*6*). Functional MRI data were slice-time corrected using AFNI(*7*) and realigned to a mean reference image using mcflirt(*8*). Susceptibility distortion correction was performed by co-registering the functional image to the intensity-inverted T1w image with an representative EPI distortion atlas(*9*). This was followed by co-registration to the corresponding T1w using boundary-based registration, implemented using FreeSurfer's BBRegister. The motion-correcting transformations, field-distortion-correcting warp, BOLD-to-T1w transformation, and T1w-to-MNI warp were concatenated and applied in a single step using ANTS. ICA-based Automatic Removal Of Motion Artifacts (AROMA) was used to generate signal and noise and signal regressors for use in the non-aggressive variant of the method(*10*). Regressors were calculated on the spatially smoothed output 6 mm FWHM kernel) and then applied to the unsmoothed pre-processed file. Following ICA-AROMA, we extracted mean time courses from eroded masks of the WM and CSF and regressed these signals out of the ICA-AROMA denoised data. Finally, each dataset was detrended with a 2nd order polynomial and high-pass filtered at 0.005 Hz using AFNI's 3dTproject. The mean

global signal was extracted using a whole-brain mask and was regressed out of each dataset. Further details on processing, denoising and quality control, please see are reported elsewhere(*11*).

Both the HCP-EP and TCP datasets were acquired use the Human Connectome Project (HCP) MRI acquisition parameters. We therefore implemented the Minimal Processing Pipeline which was developed and optimized for HCP data(*12*). The pipeline adapts steps from FMRIB Software Library ((FSL; *13*)) and FreeSurfer to account for greater spatial and temporal resolution and HCP-data related distortions resulting from acquisition choices such as multiband acceleration, while aiming to remove the least amount of data necessary. During this pipeline, brain surfaces were reconstructed using recon-all from FreeSurfer v6. Skull stripped T1w and fMRI data were aligned using FSL Linear Image Registration Tool (FLIRT). Spin Echo EPI Field Maps with opposite phase encoding directions were used to estimate spatial distortion, using FSL topup and FLIRT was used to correct the scans for such distortions. This process was fine-tuned and optimised using FreeSurfer's BBRegister. Functional MRI data realigned to a mean reference image using mcflirt(*8*). Lastly, non-linear registration of Functional MRI data, aligned to individual's structural volume space into standard MNI152 space was done using FLIRT and FMRIB's nonlinear image registration tool (FNIRT). To denoise the fMRI data, ICA-FIX was implemented. During ICA-FIX, the fMRI data is decomposed into spatially independent components using Multivariate Exploratory Linear Optimized Decomposition into Independent Components (MELODIC). The resulting components are then classified as noise or signal. While ICA-AROMA uses a set of fixed rules depending on the time-course and frequency of each component, ICA-FIX uses a machine-learning based classifier. Here we used the pre-trained HCP_hp2000 classifier provided with ICA-FIX(*2*), as the acquisition parameters of the fMRI data this classifier was train on are identical to those of the HCP-EP and TCP datasets. A temporal high-pass filter of 2000 was applied and a lenient threshold component labelling in FIX (t=10) was used. Finally, the mean global signal was extracted using a whole-brain mask and was regressed out of each dataset.

The steps described above resulted in processed and denoised fMRI dataset in MNI152 volume space for each individual. For each fMRI dataset, the time series were averaged within each of the 400 cortical(*14*) and 19 subcortical(*15*) parcels and pairwise Pearson's correlations were computed to generate a 419×419 functional connectivity matrix, after which correlation values were z-scored and the upper-triangle of this matrix which consisted of 87,571 unique functional connectivity estimates were entered into the prediction models.

Meta-matching DNN variable selection procedure

To obtain the final set of 67 phenotypes we followed the exact procedure outlined in (*16*), and began by extracting all 3,937 unique phenotypes available under UK Biobank resource application 25163. We then performed three stages of selection and processing:

Stage 1: we removed non-continuous and non-integer data fields (date and time converted to float), except for sex, brain MRI phenotypes (category ID 100), first repeat imaging visit (instance 3), first two instances (instances 0 and 1) if first imaging visit (instance 2) exists and first imaging visit (instance 2) if participants were more than double of participants from instances 0 or 1, first instance (instance 0) if only the first two instances (instances 0 and 1) exist and instance 1 participants were more than double of participants from instance 0, phenotypes for which fewer

than 2,000 participants had RSFC data, behaviors with the same value for more than 80% of participants. After the first stage of filtering, we were left with 701 phenotypes.

Stage 2: It is likely that not all phenotypes are predictable using FC. Therefore, in the second stage, our goal was to remove phenotypes that could not be predicted accurately even with a large number of participants. Therefore, we randomly selected 1,000 participants from 37,848 participants. These 1,000 participants were completely excluded from the main experiments. Using these 1,000 participants, KRR was used to predict each of the 701 phenotypes using RSFC. To ensure robustness, we performed 100 random repeats of training, validation, and testing (60%, 20%, and 20%, respectively). For each repeat, KRR was trained on the training set, and hyperparameters were tuned on the validation set. We then evaluated the trained KRR on the test set. Phenotypes with an average test prediction performance (Pearson's correlation) less than 0.1 were removed. At the end of this second stage, 265 phenotypes were left. See (*16*)for a list of selected and removed UK Biobank phenotypes.

Stage 3: Many of the remaining phenotypes were highly correlated. PCA was performed separately on each subgroup of highly similar phenotypes in the 1,000-participant sample. Similarity was evaluated based on the UK Biobank-provided categories of item sets (that is, items under the same category were considered highly similar). PCAs were not applied to 18 phenotypes (out of 265 phenotypes), which were not similar to other phenotypes. For the purpose of carrying out PCA, missing values were filled in using the expectation–maximization algorithm. For each PCA, we kept enough components to explain 95% of the variance in the data or six components, whichever was lower. Overall, the PCA step reduced the 247 phenotypes (out of 265 phenotypes) to 93 phenotypes. We then repeated the previous step (stage 2) on these 93 phenotypes, resulting in 49 phenotypes with prediction performance (Pearson's correlation) larger than 0.1. Adding back the 18 phenotypes that were not processed by PCA, we ended up with 67 phenotypes used in this manuscript.

The final list of the phenotypes and a brief description of each variable can be found in in Supplementary Table 3.

REFERENCES AND NOTES

1. R. A. Poldrack, G. Huckins, G. Varoquaux, Establishment of best practices for evidence for prediction: A review. *JAMA Psychiatry* **77**, 534–540 (2020).

2. G. Varoquaux, Cross-validation failure: Small sample sizes lead to large error bars. *Neuroimage* **180**, 68–77 (2018).

3. R. Whelan, H. Garavan, When optimism hurts: Inflated predictions in psychiatric neuroimaging. *Biol. Psychiatry* **75**, 746–748 (2014).

4. A. Abramovitch, T. Short, A. Schweiger, The C Factor: Cognitive dysfunction as a transdiagnostic dimension in psychopathology. *Clin. Psychol. Rev.* **86**, 102007 (2021).

5. C. East-Richard, A. R. Mercier, D. Nadeau, C. Cellard, Transdiagnostic neurocognitive deficits in psychiatry: A review of meta-analyses. *Can. Psychol.* **61**, 190–214 (2020).

6. L. M. McTeague, M. S. Goodkind, A. Etkin, Transdiagnostic impairment of cognitive control in mental illness. *J. Psychiatr. Res.* **83**, 37–46 (2016).

7. M. J. Millan, Y. Agid, M. Brüne, E. T. Bullmore, C. S. Carter, N. S. Clayton, R. Connor, S. Davis, B. Deakin, R. J. DeRubeis, B. Dubois, M. A. Geyer, G. M. Goodwin, P. Gorwood, T. M. Jay, M. Joëls, I. M. Mansuy, A. Meyer-Lindenberg, D. Murphy, E. Rolls, B. Saletu, M. Spedding, J. Sweeney, M. Whittington, L. J. Young, Cognitive dysfunction in psychiatric disorders: Characteristics, causes and the quest for improved therapy. *Nat. Rev. Drug Discov.* **11**, 141–168 (2012).

8. C. Shilyansky, L. M. Williams, A. Gyurak, A. Harris, T. Usherwood, A. Etkin, Effect of antidepressant treatment on cognitive impairments associated with depression: A randomised longitudinal study. *Lancet Psychiatry* **3**, 425–435 (2016).

9. S. Mohamed, R. Rosenheck, M. Swartz, S. Stroup, J. A. Lieberman, R. S. Keefe, Relationship of cognition and psychopathology to functional impairment in schizophrenia. *Am. J. Psychiatry* **165**, 978–987 (2008).

10. M. F. Green, Cognitive impairment and functional outcome in schizophrenia and bipolar disorder. *J. Clin. Psychiatry* **67**, 3 (2006).

11. A. Diamond, Executive functions. *Annu. Rev. Psychol.* **64**, 135–168 (2013).

12. H. M. Fitzgerald, J. Shepherd, H. Bailey, M. Berry, J. Wright, M. Chen, Treatment goals in schizophrenia: A real-world survey of patients, psychiatrists, and caregivers in the United States, with an analysis of current treatment (long-acting injectable vs oral antipsychotics) and goal selection. *Neuropsychiatr. Dis. Treat.* **17**, 3215–3228 (2021).

13. E. C. McNaughton, C. Curran, J. Granskie, M. Opler, S. Sarkey, L. Mucha, A. Eramo, C. Francois, B. Webber-Lind, M. McCue, Patient attitudes toward and goals for MDD treatment: A survey study. *Patient Prefer. Adherence* **13**, 959–967 (2019).

14. C. H. Xia, Z. Ma, R. Ciric, S. Gu, R. F. Betzel, A. N. Kaczkurkin, M. E. Calkins, P. A. Cook, A. García de la Garza, S. N. Vandekar, Z. Cui, T. M. Moore, D. R. Roalf, K. Ruparel, D. H. Wolf, C. Davatzikos, R. C. Gur, R. E. Gur, R. T. Shinohara, D. S. Bassett, T. D. Satterthwaite, Linked dimensions of psychopathology and connectivity in functional brain networks. *Nat. Commun.* **9**, 3003 (2018).

15. M. L. Elliott, A. Romer, A. R. Knodt, A. R. Hariri, A connectome-wide functional signature of transdiagnostic risk for mental illness. *Biol. Psychiatry* **84**, 452–459 (2018).

16. L. D. Vanes, R. J. Dolan, Transdiagnostic neuroimaging markers of psychiatric risk: A narrative review. *Neuroimage* **30**, 102634 (2021).

17. A. Anticevic, M. W. Cole, J. D. Murray, P. R. Corlett, X.-J. Wang, J. H. Krystal, The role of default network deactivation in cognition and disease. *Trends Cogn. Sci.* **16**, 584–592 (2012).

18. S. Chopra, S. M. Francey, B. O'Donoghue, K. Sabaroedin, A. Arnatkeviciute, V. Cropley, B. Nelson, J. Graham, L. Baldwin, S. Tahtalian, H. P. Yuen, K. Allott, M. Alvarez-Jimenez, S. Harrigan, C. Pantelis, S. J. Wood, P. McGorry, A. Fornito, Functional connectivity in antipsychotic-treated and antipsychotic-naive patients with first-episode psychosis and low

risk of self-harm or aggression: A secondary analysis of a randomized clinical trial. *JAMA Psychiatry* **78**, 994–1004 (2021).

19. J. L. Vincent, I. Kahn, A. Z. Snyder, M. E. Raichle, R. L. Buckner, Evidence for a frontoparietal control system revealed by intrinsic functional connectivity. *J. Neurophysiol.* **100**, 3328–3342 (2008).

20. C.-C. Huang, Q. Luo, L. Palaniyappan, A. C. Yang, C.-C. Hung, K.-H. Chou, C.-Y. Z. Lo, M.-N. Liu, S.-J. Tsai, D. M. Barch, J. Feng, C. P. Lin, T. W. Robbins, Transdiagnostic and illness-specific functional dysconnectivity across schizophrenia, bipolar disorder, and major depressive disorder. *Biol. Psychiatry Cogn. Neurosci. Neuroimaging* **5**, 542–553 (2020).

21. A. Fornito, J. Yoon, A. Zalesky, E. T. Bullmore, C. S. Carter, General and specific functional connectivity disturbances in first-episode schizophrenia during cognitive control performance. *Biol. Psychiatry* **70**, 64–72 (2011).

22. J. T. Baker, D. G. Dillon, L. M. Patrick, J. L. Roffman, R. O. Brady, D. A. Pizzagalli, D. Öngür, A. J. Holmes, Functional connectomics of affective and psychotic pathology. *Proc. Natl. Acad. Sci. U.S.A.* **116**, 9050–9059 (2019).

23. E. Dhamala, K. W. Jamison, A. Jaywant, S. Dennis, A. Kuceyeski, Distinct functional and structural connections predict crystallised and fluid cognition in healthy adults. *Hum. Brain Mapp.* **42**, 3102–3118 (2021).

24. T. He, R. Kong, A. J. Holmes, M. Nguyen, M. R. Sabuncu, S. B. Eickhoff, D. Bzdok, J. Feng, B. T. Yeo, Deep neural networks and kernel regression achieve comparable accuracies for functional connectivity prediction of behavior and demographics. *Neuroimage* **206**, 116276 (2020).

25. C. Sripada, S. Rutherford, M. Angstadt, W. K. Thompson, M. Luciana, A. Weigard, L. H. Hyde, M. Heitzeg, Prediction of neurocognition in youth from resting state fMRI. *Mol. Psychiatry* **25**, 3413–3421 (2020).

26. E. S. Finn, X. Shen, D. Scheinost, M. D. Rosenberg, J. Huang, M. M. Chun, X. Papademetris, R. T. Constable, Functional connectome fingerprinting: Identifying individuals using patterns of brain connectivity. *Nat. Neurosci.* **18**, 1664–1671 (2015).

27. R. Jiang, V. D. Calhoun, L. Fan, N. Zuo, R. Jung, S. Qi, D. Lin, J. Li, C. Zhuo, M. Song, Z. Fu, T. Jiang, J. Sui, Gender differences in connectome-based predictions of individualized intelligence quotient and sub-domain scores. *Cereb. Cortex* **30**, 888–900 (2020).

28. S. Marek, B. Tervo-Clemmens, F. J. Calabro, D. F. Montez, B. P. Kay, A. S. Hatoum, M. R. Donohue, W. Foran, R. L. Miller, T. J. Hendrickson, S. M. Malone, S. Kandala, E. Feczko, O. Miranda-Dominguez, A. M. Graham, E. A. Earl, A. J. Perrone, M. Cordova, O. Doyle, L. A. Moore, G. M. Conan, J. Uriarte, K. Snider, B. J. Lynch, J. C. Wilgenbusch, T. Pengo, A. Tam, J. Chen, D. J. Newbold, A. Zheng, N. A. Seider, A. N. Van, A. Metoki, R. J. Chauvin, T. O. Laumann, D. J. Greene, S. E. Petersen, H. Garavan, W. K. Thompson, T. E. Nichols, B. T. T. Yeo, D. M. Barch, B. Luna, D. A. Fair, N. U. F. Dosenbach, Reproducible brain-wide association studies require thousands of individuals. *Nature* **603**, 654–660 (2022).

29. M.-A. Schulz, B. Yeo, J. T. Vogelstein, J. Mourao-Miranada, J. N. Kather, K. Kording, B. Richards, D. Bzdok, Different scaling of linear models and deep learning in UKBiobank brain images versus machine-learning datasets. *Nat. Commun.* **11**, 4238 (2020).

30. M. Helmer, S. Warrington, A.-R. Mohammadi-Nejad, J. L. Ji, A. Howell, B. Rosand, A. Anticevic, S. N. Sotiropoulos, J. D. Murray, On the stability of canonical correlation analysis and partial least squares with application to brain-behavior associations. *Commun. Biol.* **7**, 217 (2024).

31. S. Haufe, F. Meinecke, K. Görgen, S. Dähne, J.-D. Haynes, B. Blankertz, F. Bießmann, On the interpretation of weight vectors of linear models in multivariate neuroimaging. *Neuroimage* **87**, 96–110 (2014).

32. F. Váša, B. Mišić, Null models in network neuroscience. *Nat. Rev. Neurosci.* **23**, 493–504 (2022).

33. L. Tozzi, S. L. Fleming, Z. D. Taylor, C. D. Raterink, L. M. Williams, Test-retest reliability of the human functional connectome over consecutive days: Identifying highly reliable portions and assessing the impact of methodological choices. *Netw. Neurosci.* **4**, 925–945 (2020).

34. X.-N. Zuo, X.-X. Xing, Test-retest reliabilities of resting-state FMRI measurements in human brain functional connectomics: A systems neuroscience perspective. *Neurosci. Biobehav. Rev.* **45**, 100–118 (2014).

35. S. M. Smith, T. E. Nichols, D. Vidaurre, A. M. Winkler, T. E. Behrens, M. F. Glasser, K. Ugurbil, D. M. Barch, D. C. Van Essen, K. L. Miller, A positive-negative mode of population covariation links brain connectivity, demographics and behavior. *Nat. Neurosci.* **18**, 1565–1567 (2015).

36. J. Chen, A. Tam, V. Kebets, C. Orban, L. Q. R. Ooi, C. L. Asplund, S. Marek, N. U. Dosenbach, S. B. Eickhoff, D. Bzdok, A. J. Holmes, B. T. T. Yeo, Shared and unique brain network features predict cognitive, personality, and mental health scores in the ABCD study. *Nat. Commun.* **13**, 1–17 (2022).

37. K. L. Miller, F. Alfaro-Almagro, N. K. Bangerter, D. L. Thomas, E. Yacoub, J. Xu, A. J. Bartsch, S. Jbabdi, S. N. Sotiropoulos, J. L. Andersson, L. Griffanti, G. Douaud, T. W. Okell, P. Weale, I. Dragonu, S. Garratt, S. Hudson, R. Collins, M. Jenkinson, P. M. Matthews, S. M. Smith, Multimodal population brain imaging in the UK Biobank prospective epidemiological study. *Nat. Neurosci.* **19**, 1523–1536 (2016).

38. T. He, L. An, P. Chen, J. Chen, J. Feng, D. Bzdok, A. J. Holmes, S. B. Eickhoff, B. Yeo, Meta-matching as a simple framework to translate phenotypic predictive models from big to small data. *Nat. Neurosci.* **25**, 795–804 (2022).

39. A. Schaefer, R. Kong, E. M. Gordon, T. O. Laumann, X.-N. Zuo, A. J. Holmes, S. B. Eickhoff, B. T. T. Yeo, Local-global parcellation of the human cerebral cortex from intrinsic functional connectivity MRI. *Cereb. Cortex* **28**, 3095–3114 (2022).

40. B. Fischl, D. H. Salat, E. Busa, M. Albert, M. Dieterich, C. Haselgrove, A. Van Der Kouwe, R. Killiany, D. Kennedy, S. Klaveness, A. Montillo, N. Makris, B. Rosen, A. M. Dale, Whole

brain segmentation: Automated labeling of neuroanatomical structures in the human brain. *Neuron* **33**, 341–355 (2002).

41. L. Q. R. Ooi, J. Chen, S. Zhang, R. Kong, A. Tam, J. Li, E. Dhamala, J. H. Zhou, A. J. Holmes, B. T. Yeo, Comparison of individualized behavioral predictions across anatomical, diffusion and functional connectivity MRI. *Neuroimage* **263**, 119636 (2022).

42. Y. Tian, A. Zalesky, Machine learning prediction of cognition from functional connectivity: Are feature weights reliable? *Neuroimage* **245**, 118648 (2021).

43. J. Chen, L. Q. R. Ooi, T. W. Kiat Tan, S. Zhang, J. Li, C. L. Asplund, S. B. Eickhoff, D. Bzdok, A. J. Holmes, B. T. Yeo, Relationship between prediction accuracy and feature importance reliability: An empirical and theoretical study. *Neuroimage* **274**, 120115 (2023).

44. M. W. Cole, G. Repovš, A. Anticevic, The frontoparietal control system: A central role in mental health. *Neuroscientist* **20**, 652–664 (2014).

45. T. P. Zanto, A. Gazzaley, Fronto-parietal network: Flexible hub of cognitive control. *Trends Cogn. Sci.* **17**, 602–603 (2013).

46. J. Smallwood, K. Brown, B. Baird, J. W. Schooler, Cooperation between the default mode network and the frontal–parietal network in the production of an internal train of thought. *Brain Res.* **1428**, 60–70 (2012).

47. B. T. Yeo, F. M. Krienen, J. Sepulcre, M. R. Sabuncu, D. Lashkari, M. Hollinshead, J. L. Roffman, J. W. Smoller, L. Zöllei, J. R. Polimeni, B. Fischl, H. Liu, R. L. Buckner, The organization of the human cerebral cortex estimated by intrinsic functional connectivity. *J. Neurophysiol.* **106**, 1125–1165 (2011).

48. P. Flechsig, Die Localisation der geistigen Vorgänge insbesondere der Sinnesempfindungen des Menschen (De Gruyter, 1896).

49. P. S. Goldman-Rakic, Topography of cognition: Parallel distributed networks in primate association cortex. *Annu. Rev. Neurosci.* **11**, 137–156 (1988).

50. D. Badre, D. E. Nee, Frontal cortex and the hierarchical control of behavior. *Trends Cogn. Sci.* **22**, 170–188 (2018).

51. K. Allott, A. Lin, "Cognitive risk factors for psychosis" in *Risk Factors for Psychosis* (Elsevier, 2020), pp. 269–287.

52. A. Catalan, G. S. De Pablo, C. Aymerich, S. Damiani, V. Sordi, J. Radua, D. Oliver, P. McGuire, A. J. Giuliano, W. S. Stone, P. Fusar-Poli, Neurocognitive functioning in individuals at clinical high risk for psychosis: A systematic review and meta-analysis. *JAMA Psychiatry* **78**, 859–867 (2021).

53. X. Tong, H. Xie, N. Carlisle, G. A. Fonzo, D. J. Oathes, J. Jiang, Y. Zhang, Transdiagnostic connectome signatures from resting-state fMRI predict individual-level intellectual capacity. *Transl. Psychiatry* **12**, 367 (2022).

54. E. A. Boeke, A. J. Holmes, E. A. Phelps, Toward robust anxiety biomarkers: A machine learning approach in a large-scale sample. *Biol. Psychiatry Cogn. Neurosci. Neuroimaging* **5**, 799–807 (2020).

55. E. Dhamala, L. Q. R. Ooi, J. Chen, R. Kong, K. Anderson, R. Chin, B. T. Yeo, A. Holmes, Proportional intracranial volume correction differentially biases behavioral predictions across neuroanatomical features and populations. *Neuroimage* **260**, 119485 (2022).

56. H.-J. Park, K. Friston, Structural and functional brain networks: From connections to cognition. *Science* **342**, 1238411 (2013).

57. S. E. Petersen, O. Sporns, Brain networks and cognitive architectures. *Neuron* **88**, 207–219 (2015).

58. A. Segal, L. Parkes, K. Aquino, S. M. Kia, T. Wolfers, B. Franke, M. Hoogman, C. F. Beckmann, L. T. Westlye, O. A. Andreassen, A. Zalesky, B. J. Harrison, C. Davey, C. Soriano-Mas, N. Cardoner, J. Tiego, M. Yücel, L. Braganza, C. Suo, M. Berk, S. Cotton, M. A. Bellgrove, A. F. Marquand, A. Fornito, Regional, circuit, and network heterogeneity of brain abnormalities in psychiatric disorders. *Nat. Neurosci.* **26**, 1613–1629 (2023).

59. M. Y. Chan, “Age-related desegregation of functional systems in healthy adults: The underlying patterns of connections and protective life-course factors” thesis, The University of Texas at Dallas, Richardson, TX (2016).

60. T. S. Kong, C. Gratton, K. A. Low, C. H. Tan, A. M. Chiarelli, M. A. Fletcher, B. Zimmerman, E. L. Maclin, B. P. Sutton, G. Gratton, M. Fabiani, Age-related differences in functional brain network segregation are consistent with a cascade of cerebrovascular, structural, and cognitive effects. *Netw. Neurosci.* **4**, 89–114 (2020).

61. W. Johnson, T. J. Bouchard Jr., R. F. Krueger, M. McGue, I. I. Gottesman, Just one g: Consistent results from three test batteries. *Intelligence* **32**, 95–107 (2004).

62. C. Fawns-Ritchie, I. J. Deary, Reliability and validity of the UK Biobank cognitive tests. *PLOS ONE* **15**, e0231627 (2020).

63. J. E. Savage, P. R. Jansen, S. Stringer, K. Watanabe, J. Bryois, C. A. De Leeuw, M. Nagel, S. Awasthi, P. B. Barr, J. R. Coleman, K. L. Grasby, A. R. Hammerschlag, J. A. Kaminski, R. Karlsson, E. Krapohl, M. Lam, M. Nygaard, C. A. Reynolds, J. W. Trampush, H. Young, D. Zabaneh, S. Hägg, N. K. Hansell, I. K. Karlsson, S. Linnarsson, G. W. Montgomery, A. B. Muñoz-Manchado, E. B. Quinlan, G. Schumann, N. G. Skene, B. T. Webb, T. White, D. E. Arking, D. Avramopoulos, R. M. Bilder, P. Bitsios, K. E. Burdick, T. D. Cannon, O. Chiba-Falek, A. Christoforou, E. T. Cirulli, E. Congdon, A. Corvin, G. Davies, I. J. Deary, P. DeRosse, D. Dickinson, S. Djurovic, G. Donohoe, E. D. Conley, J. G. Eriksson, T. Espeseth, N. A. Freimer, S. Giakoumaki, I. Giegling, M. Gill, D. C. Glahn, A. R. Hariri, A. Hatzimanolis, M. C. Keller, E. Knowles, D. Koltai, B. Konte, J. Lahti, S. Le Hellard, T. Lencz, D. C. Liewald, E. London, A. J. Lundervold, A. K. Malhotra, I. Melle, D. Morris, A. C. Need, W. Ollier, A. Palotie, A. Payton, N. Pendleton, R. A. Poldrack, K. Räikkönen, I. Reinvang, P. Roussos, D. Rujescu, F. W. Sabb, M. A. Scult, O. B. Smeland, N. Smyrnis, J. M. Starr, V. M. Steen, N. C. Stefanis, R. E. Straub, K. Sundet, H. Tiemeier, A. N. Voineskos, D. R. Weinberger, E. Widen, J. Yu, G. Abecasis, O. A. Andreassen, G. Breen, L. Christiansen, B. Debrabant, D. M. Dick, A. Heinz, J. Hjerling-Leffler, M. A. Ikram, K. S. Kendler, N. G. Martin, S. E. Medland, N. L. Pedersen, R. Plomin, T. J. C. Polderman, S. Ripke, S. van der Sluis, P. F. Sullivan, S. I. Vrieze, M. J. Wright, D. Posthuma, Genome-wide association

meta-analysis in 269,867 individuals identifies new genetic and functional links to intelligence. *Nat. Genet.* **50**, 912–919 (2018).

64. S. Noble, D. Scheinost, R. T. Constable, A decade of test-retest reliability of functional connectivity: A systematic review and meta-analysis. *Neuroimage* **203**, 116157 (2019).

65. L. Q. R. Ooi, C. Orban, T. E. Nichols, S. Zhang, T. W. K. Tan, R. Kong, S. Marek, N. U. Dosenbach, T. Laumann, E. M. Gordon, J. H. Zhou, D. Bzdok, S. B. Eickhoff, A. J Holmes, B. T. T. Yeo; Alzheimer's Disease Neuroimaging Initiative, MRI economics: Balancing sample size and scan duration in brain wide association studies. bioRxiv 2024.02.16.580448 [Preprint] (2024). https://doi.org/10.1101/2024.02.16.580448.

66. J. Chen, L. Q. R. Ooi, J. Li, C. L. Asplund, S. B. Eickhoff, D. Bzdok, A. J. Holmes, B. T. Yeo, There is no fundamental trade-off between prediction accuracy and feature importance reliability. bioRxiv 2022.08.08.503167 [Preprint] (2022). https://doi.org/10.1101/2022.08.08.503167.

67. C. Bycroft, C. Freeman, D. Petkova, G. Band, L. T. Elliott, K. Sharp, A. Motyer, D. Vukcevic, O. Delaneau, J. O'Connell, A. Cortes, S. Welsh, A. Young, M. Effingham, G. McVean, S. Leslie, N. Allen, P. Donnelly, J. Marchini, The UK Biobank resource with deep phenotyping and genomic data. *Nature* **562**, 203–209 (2018).

68. K. E. Lewandowski, S. Bouix, D. Ongur, M. E. Shenton, Neuroprogression across the early course of psychosis. *J. Psychiatr. Brain Sci.* **5**, e200002 (2020).

69. S. Chopra, C. V. Cocuzza, C. Lawhead, J. A. Ricard, L. Labache, L. M. Patrick, P. Kumar, A. Rubenstein, J. Moses, L. Chen, C. Blankenbaker, B. Gillis, L. T. Germine, I. Harpaz-Rote, B. T. T. Yeo, J. T. Baker, A. J. Holmes, The Transdiagnostic Connectome Project: A richly phenotyped open dataset for advancing the study of brain-behavior relationships in psychiatry. medRxiv 2024.06.18.24309054 [Preprint] (2024). https://doi.org/10.1101/2024.06.18.24309054.

70. R. A. Poldrack, E. Congdon, W. Triplett, K. Gorgolewski, K. Karlsgodt, J. Mumford, F. Sabb, N. Freimer, E. London, T. Cannon, R. M. Bilder, A phenome-wide examination of neural and cognitive function. *Sci. Data* **3**, 1–12 (2016).

71. J. D. Power, C. J. Lynch, B. M. Silver, M. J. Dubin, A. Martin, R. M. Jones, Distinctions among real and apparent respiratory motions in human fMRI data. *Neuroimage* **201**, 116041 (2019).

72. D. A. Fair, O. Miranda-Dominguez, A. Z. Snyder, A. Perrone, E. A. Earl, A. N. Van, J. M. Koller, E. Feczko, M. D. Tisdall, A. van der Kouwe, R. L. Klein, A. E. Mirro, J. M. Hampton, B. Adeyemo, T. O. Laumann, C. Gratton, D. J. Greene, B. L. Schlaggar, D. J. Hagler Jr., R. Watts, H. Garavan, D. M. Barch, J. T. Nigg, S. E. Petersen, A. M. Dale, S. W. Feldstein-Ewing, B. J. Nagel, N. U. F. Dosenbach, Correction of respiratory artifacts in MRI head motion estimates. *Neuroimage* **208**, 116400 (2020).

73. J. D. Power, A. Mitra, T. O. Laumann, A. Z. Snyder, B. L. Schlaggar, S. E. Petersen, Methods to detect, characterize, and remove motion artifact in resting state fMRI. *Neuroimage* **84**, 320–341 (2014).

74. L. Parkes, B. Fulcher, M. Yücel, A. Fornito, An evaluation of the efficacy, reliability, and sensitivity of motion correction strategies for resting-state functional MRI. *Neuroimage* **171**, 415–436 (2018).

75. J. Li, R. Kong, R. Liégeois, C. Orban, Y. Tan, N. Sun, A. J. Holmes, M. R. Sabuncu, T. Ge, B. T. Yeo, Global signal regression strengthens association between resting-state functional connectivity and behavior. *Neuroimage* **196**, 126–141 (2019).

76. S. Weintraub, S. S. Dikmen, R. K. Heaton, D. S. Tulsky, P. D. Zelazo, P. J. Bauer, N. E. Carlozzi, J. Slotkin, D. Blitz, K. Wallner-Allen, N. A. Fox, J. L. Beaumont, D. Mungas, C. J. Nowinski, J. Richler, J. A. Deocampo, J. E. Anderson, J. J. Manly, B. Borosh, R. Havlik, K. Conway, E. Edwards, L. Freund, J. W. King, C. Moy, E. Witt, R. C. Gershon, Cognition assessment using the NIH Toolbox. *Neurology* **80**, S54–S64 (2013).

77. D. Wechsler, Wechsler Abbreviated Scale of Intelligence (Pearson Education, 1999).

78. S. Singh, R. W. Strong, L. Jung, F. H. Li, L. Grinspoon, L. S. Scheuer, E. J. Passell, P. Martini, N. Chaytor, J. R. Soble, The TestMyBrain digital neuropsychology toolkit: Development and psychometric characteristics. *J. Clin. Exp. Neuropsychol.* **43**, 786–795 (2021).

79. D. Wechsler, *Wechsler Memory Scale* (Psychological Corporation, 1945).

80. D. Wechsler, *Wechsler Adult Intelligence Scale*, Archives of Clinical Neuropsychology (Psychological Corporation, 1955).

81. E. Dhamala, L. Q. R. Ooi, J. Chen, J. A. Ricard, E. Berkeley, S. Chopra, Y. Qu, C. Lawhead, B. T. T. Yeo, A. J. Holmes, Brain-based predictions of psychiatric illness-linked behaviors across the sexes. *Biol. Psychiatry.* **94**, 479–491 (2022).

82. R. X. Rodriguez, S. Noble, C. C. Camp, D. Scheinost, Connectome caricatures: Removing large-amplitude co-activation patterns in resting-state fMRI emphasizes individual differences. bioRxiv 2024.04.08.588578 [Preprint] (2024). https://doi.org/10.1101/2024.04.08.588578.

83. A. Mihalik, M. Brudfors, M. Robu, F. S. Ferreira, H. Lin, A. Rau, T. Wu, S. B. Blumberg, B. Kanber, M. Tariq, "ABCD neurocognitive prediction challenge 2019: Predicting individual fluid intelligence scores from structural MRI using probabilistic segmentation and kernel ridge regression" in *Challenge in Adolescent Brain Cognitive Development Neurocognitive Prediction* (Springer, 2019), pp. 133–142.

84. P. Chen, L. An, N. Wulan, C. Zhang, S. Zhang, L. Q. R. Ooi, R. Kong, J. Chen, J. Wu, S. Chopra, D. Bzdok, S. B. Eickhoff, A. J. Holmes, B. T. T. Yeo, Multilayer meta-matching: Translating phenotypic prediction models from multiple datasets to small data. bioRxiv 2023.12.05.569848 [Preprint] (2023). https://doi.org/10.1101/2023.12.05.569848.

85. T. E. Raghunathan, R. Rosenthal, D. B. Rubin, Comparing correlated but nonoverlapping correlations. *Psychol. Methods* **1**, 178–183 (1996).

86. B. Diedenhofen, J. Musch, cocor: A comprehensive solution for the statistical comparison of correlations. *PLOS ONE* **10**, e0121945 (2015).

87. E. Dhamala, B. T. Yeo, A. J. Holmes, One size does not fit all: Methodological considerations for brain-based predictive modeling in psychiatry. *Biol. Psychiatry* **93**, 717–728 (2023).

88. D. Chyzhyk, G. Varoquaux, M. Milham, B. Thirion, How to remove or control confounds in predictive models, with applications to brain biomarkers. *Gigascience* **11**, giac014 (2022).

89. F. Alfaro-Almagro, M. Jenkinson, N. K. Bangerter, J. L. Andersson, L. Griffanti, G. Douaud, S. N. Sotiropoulos, S. Jbabdi, M. Hernandez-Fernandez, E. Vallee, D. Vidaurre, M. Webster, P. McCarthy, C. Rorden, A. Daducci, D. C. Alexander, H. Zhang, I. Dragonu, P. M. Matthews, K. L. Miller, S. M. Smith, Image processing and Quality Control for the first 10,000 brain imaging datasets from UK Biobank. *Neuroimage* **166**, 400–424 (2018).

90. G. Salimi-Khorshidi, G. Douaud, C. F. Beckmann, M. F. Glasser, L. Griffanti, S. M. Smith, Automatic denoising of functional MRI data: Combining independent component analysis and hierarchical fusion of classifiers. *Neuroimage* **90**, 449–468 (2014).

91. O. Esteban, C. J. Markiewicz, R. W. Blair, C. A. Moodie, A. I. Isik, A. Erramuzpe, J. D. Kent, M. Goncalves, E. DuPre, M. Snyder, H. Oya, S. S. Ghosh, J. Wright, J. Durnez, R. A. Poldrack, K. J. Gorgolewski, fMRIPrep: A robust preprocessing pipeline for functional MRI. *Nat. Methods* **16**, 111–116 (2019).

92. N. J. Tustison, B. B. Avants, P. A. Cook, Y. Zheng, A. Egan, P. A. Yushkevich, J. C. Gee, N4ITK: Improved N3 bias correction. *IEEE Trans. Med. Imaging* **29**, 1310–1320 (2010).

93. B. B. Avants, N. Tustison, G. Song, Advanced normalization tools (ANTS). *Insight J.* **2**, 1–35 (2009).

94. Y. Zhang, M. Brady, S. Smith, Segmentation of brain MR images through a hidden Markov random field model and the expectation-maximization algorithm. *IEEE Trans. Med. Imaging* **20**, 45–57 (2001).

95. R. W. Cox, AFNI: Software for analysis and visualization of functional magnetic resonance neuroimages. *Comput. Biomed. Res.* **29**, 162–173 (1996).

96. M. Jenkinson, P. Bannister, M. Brady, S. Smith, Improved optimization for the robust and accurate linear registration and motion correction of brain images. *Neuroimage* **17**, 825–841 (2002).

97. S. Wang, D. J. Peterson, J. C. Gatenby, W. Li, T. J. Grabowski, T. M. Madhyastha, Evaluation of field map and nonlinear registration methods for correction of susceptibility artifacts in diffusion MRI. *Front. Neuroinform.* **11**, 17 (2017).

98. R. H. R. Pruim, M. Mennes, D. van Rooij, A. Llera, J. K. Buitelaar, C. F. Beckmann, ICA-AROMA: A robust ICA-based strategy for removing motion artifacts from fMRI data. *Neuroimage* **112**, 267–277 (2015).

99. K. M. Aquino, B. D. Fulcher, L. Parkes, K. Sabaroedin, A. Fornito, Identifying and removing widespread signal deflections from fMRI data: Rethinking the global signal regression problem. *Neuroimage* **212**, 116614 (2020).

100. M. F. Glasser, S. N. Sotiropoulos, J. A. Wilson, T. S. Coalson, B. Fischl, J. L. Andersson, J. Xu, S. Jbabdi, M. Webster, J. R. Polimeni, D. C. Van Essen, M. Jenkinson, WU-Minn HCP Consortium, The minimal preprocessing pipelines for the Human Connectome Project. *Neuroimage* **80**, 105–124 (2013).

101. M. Jenkinson, C. F. Beckmann, T. E. Behrens, M. W. Woolrich, S. M. Smith, FSL. *Neuroimage* **62**, 782–790 (2012).